

Reverse design of high-detonation-velocity organic energetic compounds based on an accurate BPNN with wide applicability

Qiong Wu^{a,b,c,#}, Guan-chen Dong^{a,b,#}, Shuai-yu Wang^{a,b}, Xin-yu Wang^{a,b}, Bin Yan^a, Wei-hua Zhu^a,

Jing Lv^{a,b,*}, Ling-hua Tan^{a,b,*}

^a School of Chemistry and Chemical Engineering, Nanjing University of Science and Technology, Nanjing 210094, China

^b National Special Superfine Powder Engineering Research Center, Nanjing University of Science and Technology, Nanjing 210014, China

^c School of Materials Science and Engineering, Jiangsu Key Laboratory of Advanced Structural Materials and Application Technology, Nanjing Institute of Technology, Nanjing 211167, China

Qiong Wu and Guan-chen Dong contributed equally to this paper;

*Corresponding author: Ling-hua Tan and Jing Lv;

Email address: tanlh@njust.edu.cn (Ling-hua Tan) and lvjing9487@163.com (Jing Lv)

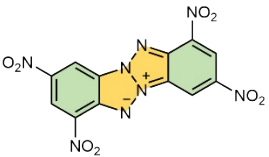
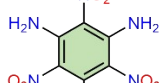
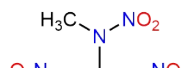
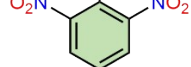
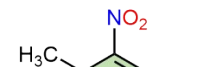
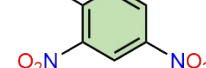
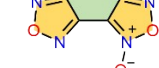
Supplementary Information

Table S1: The initial dataset for the ML; Table S2: The Pearson's correlation coefficients of descriptors for detonation velocity (D); Table S3: The setting of the RF model; Table S4: The setting of the SVR model; Table S5: The setting of the MLP model; Table S6: The setting of the BPNN model; Table S7: The predicted D values of compounds in the test set; Table S8: The dataset of new test set 1; Table S9: The new dataset of new modified ML model; Table S10: The dataset of new energetic compounds; Table S11: The predicted D values of isomers; Figure S1: The loss function of ML models; Figure S2: The relationships between nC/V_m , nH/V_m , V_m , M , OB, F and experimental D ; Figure S3: The scatter graph of the training/test set; Figure S4: The predicted residual plot of models for the D ; Figure S5: The Williams plot of models for the test set of the D .

Table S1. The initial dataset for the ML.¹

NO.	Structure	ρ	nO/ V_m	nN/ V_m	nC/ V_m	nH/ V_m	V_m	M	OB	F
Training set										
1		1.64	0.045	0.026	0.045	0.011	532.90	874.0	-0.494	5.47
2		1.78	0.049	0.029	0.049	0.012	490.99	874.0	-0.494	5.47
3		1.80	0.044	0.037	0.044	0.037	135.02	243.0	-0.560	4.83
4		1.43	0.035	0.029	0.035	0.029	170.32	243.0	-0.560	4.83
5		1.38	0.034	0.028	0.034	0.028	176.37	243.0	-0.560	4.83
6		1.38	0.049	0.014	0.028	0.056	142.05	196.0	-0.408	5.86
7		1.76	0.047	0.031	0.047	0.023	257.97	454.0	-0.529	5.22
8		1.55	0.044	0.025	0.038	0.038	158.73	246.0	-0.520	5.15
9		1.48	0.042	0.024	0.036	0.036	166.24	246.0	-0.520	5.15
10		1.63	0.046	0.027	0.040	0.040	150.94	246.0	-0.520	5.15
11		1.89	0.051	0.051	0.026	0.051	156.66	296.1	-0.216	6.08
12		1.60	0.043	0.043	0.022	0.043	185.05	296.1	-0.216	6.08
13		1.40	0.038	0.038	0.019	0.038	211.49	296.1	-0.216	6.08
14		1.20	0.032	0.032	0.016	0.032	246.73	296.1	-0.216	6.08
15		1.00	0.027	0.027	0.014	0.027	296.08	296.1	-0.216	6.08
16		0.75	0.020	0.020	0.010	0.020	394.77	296.1	-0.216	6.08
17		1.60	0.042	0.028	0.042	0.014	282.50	452.0	-0.496	5.27
18		1.60	0.043	0.021	0.050	0.021	281.25	450.0	-0.676	5.21
19		1.70	0.045	0.023	0.053	0.023	264.71	450.0	-0.676	5.21

20		1.60	0.063	0.021	0.021	0.035	141.87	227.0	0.035	7.29
21		1.70	0.048	0.024	0.048	0.013	373.51	635.0	-0.517	5.64
22		1.78	0.034	0.068	0.017	0.068	58.46	104.1	-0.308	4.20
23		1.62	0.031	0.062	0.016	0.062	64.23	104.1	-0.308	4.20
24		1.55	0.030	0.060	0.015	0.060	67.14	874.0	-0.308	4.20
25		1.55	0.030	0.060	0.015	0.060	67.14	874.0	-0.308	4.20
26		1.76	0.067	0.022	0.028	0.045	179.55	243.0	-0.101	6.92
27		1.70	0.065	0.022	0.027	0.043	185.88	243.0	-0.101	6.92
28		1.67	0.063	0.021	0.026	0.042	189.22	243.0	-0.101	6.92
29		1.60	0.061	0.020	0.025	0.041	197.50	104.1	-0.101	6.92
30		1.45	0.055	0.018	0.023	0.037	217.93	104.1	-0.101	6.92
31		1.23	0.047	0.016	0.019	0.031	256.91	316.0	-0.101	6.92
32		0.99	0.038	0.013	0.016	0.025	319.19	316.0	-0.101	6.92
33		0.88	0.033	0.011	0.014	0.022	359.09	316.0	-0.101	6.92
34		0.50	0.019	0.006	0.008	0.013	632.00	316.0	-0.101	6.92
35		0.48	0.018	0.006	0.008	0.012	658.33	316.0	-0.101	6.92
36		0.30	0.011	0.004	0.005	0.008	1053.33	316.0	-0.101	6.92
37		0.25	0.009	0.003	0.004	0.006	1264.00	316.0	-0.101	6.92
38		1.76	0.054	0.023	0.046	0.023	130.11	316.0	-0.454	5.61
39		1.71	0.052	0.022	0.045	0.022	133.91	316.0	-0.454	5.61
40		1.60	0.049	0.021	0.042	0.021	143.12	316.0	-0.454	5.61
41		1.70	0.052	0.022	0.045	0.022	134.70	316.0	-0.454	5.61
42		1.80	0.049	0.049	0.024	0.049	123.37	316.0	-0.216	6.08
43		1.77	0.048	0.048	0.024	0.048	125.46	229.0	-0.216	6.08
44		1.77	0.048	0.048	0.024	0.048	125.81	229.0	-0.216	6.08
45		1.72	0.046	0.046	0.023	0.046	129.10	229.0	-0.216	6.08
46		1.70	0.046	0.046	0.023	0.046	130.62	229.0	-0.216	6.08

47		1.66	0.045	0.045	0.022	0.045	133.77	222.1	-0.216	6.08
48		1.60	0.043	0.043	0.022	0.043	138.79	222.1	-0.216	6.08
49		1.46	0.039	0.039	0.020	0.039	152.10	222.1	-0.216	6.08
50		1.40	0.038	0.038	0.019	0.038	158.61	222.1	-0.216	6.08
51		1.29	0.035	0.035	0.017	0.035	172.14	222.1	-0.216	6.08
52		1.20	0.032	0.032	0.016	0.032	185.05	222.1	-0.216	6.08
53		1.10	0.030	0.030	0.015	0.030	201.87	222.1	-0.216	6.08
54		1.00	0.027	0.027	0.014	0.027	222.06	222.1	-0.216	6.08
55		0.95	0.026	0.026	0.013	0.026	233.75	222.1	-0.216	6.08
56		0.70	0.019	0.019	0.009	0.019	317.23	222.1	-0.216	6.08
57		0.56	0.015	0.015	0.008	0.015	396.54	222.1	-0.216	6.08
58		1.85	0.038	0.038	0.057	0.019	209.75	388.0	-0.742	4.08
59		1.88	0.044	0.044	0.044	0.044	137.27	258.1	-0.558	4.52
60		1.85	0.043	0.043	0.043	0.043	139.49	258.1	-0.558	4.52
61		1.73	0.048	0.030	0.042	0.030	165.91	287.0	-0.474	5.70
62		1.71	0.048	0.030	0.042	0.030	167.85	287.0	-0.474	5.70
63		1.68	0.047	0.029	0.041	0.029	170.85	287.0	-0.474	5.70
64		1.61	0.045	0.028	0.039	0.028	178.27	287.0	-0.474	5.70
65		1.36	0.038	0.024	0.033	0.024	211.04	287.0	-0.474	5.70
66		1.20	0.033	0.021	0.029	0.021	239.18	287.0	-0.474	5.70
67		1.64	0.043	0.022	0.051	0.036	138.43	227.0	-0.740	5.11
68		1.45	0.038	0.019	0.045	0.032	156.57	227.0	-0.740	5.11
69		1.36	0.036	0.018	0.042	0.030	166.93	227.0	-0.740	5.11
70		1.00	0.026	0.013	0.031	0.022	227.02	227.0	-0.740	5.11
71		0.80	0.021	0.011	0.025	0.018	283.78	227.0	-0.740	5.11
72		0.73	0.019	0.010	0.023	0.016	310.14	227.0	-0.740	5.11
73		1.86	0.044	0.044	0.044	0.000	135.48	252.0	-0.381	-0.30
74		1.76	0.042	0.042	0.042	0.000	143.18	252.0	-0.381	-0.30

75		1.97	0.068	0.034	0.034	0.000	176.62	347.9	0.000	6.91
76		1.74	0.031	0.062	0.031	0.000	193.14	336.1	-0.286	3.58
77		1.62	0.043	0.043	0.022	0.065	92.63	150.1	-0.320	5.91
78		1.51	0.026	0.052	0.026	0.052	115.06	174.1	-0.551	-0.43
79		1.79	0.060	0.037	0.022	0.037	133.75	239.0	-0.033	6.72
80		1.66	0.047	0.023	0.047	0.023	128.16	213.0	-0.563	5.57
Test set										
1		1.77	0.064	0.028	0.028	0.028	217.58	386.0	-0.041	6.25
2		1.68	0.048	0.021	0.048	0.035	144.65	243.0	-0.625	5.19
3		1.72	0.045	0.030	0.045	0.030	132.57	228.0	-0.561	5.17
4		1.57	0.045	0.019	0.045	0.032	154.78	243.0	-0.625	5.19

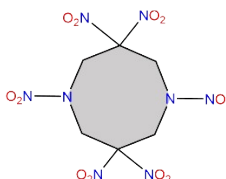
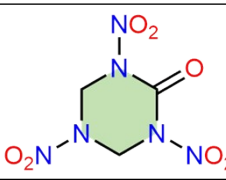
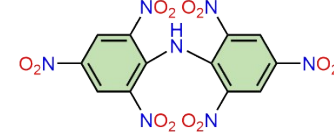
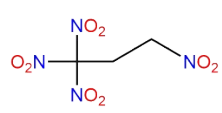
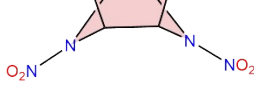
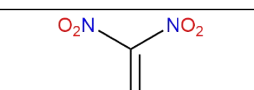
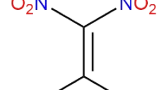
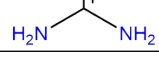
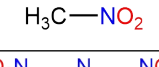
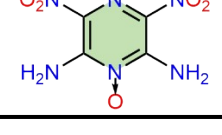
5		1.85	0.058	0.038	0.029	0.038	208.15	384.0	-0.167	6.31
6		1.85	0.055	0.047	0.023	0.031	127.93	236.0	-0.068	6.19
7		1.59	0.043	0.025	0.043	0.018	276.10	439.0	-0.528	5.42
8		1.68	0.060	0.030	0.022	0.030	133.49	224.0	0.000	6.86
9		1.93	0.053	0.053	0.026	0.026	226.97	438.1	-0.110	6.25
10		1.86	0.051	0.051	0.025	0.025	235.52	438.1	-0.110	6.25
11		1.33	0.036	0.036	0.018	0.018	330.11	438.1	-0.110	6.25
12		1.88	0.051	0.051	0.025	0.051	78.74	148.0	-0.216	5.07
13		1.78	0.048	0.048	0.024	0.048	83.17	148.0	-0.216	5.07
14		1.13	0.037	0.018	0.018	0.055	54.10	61.0	-0.393	6.04
15		1.91	0.044	0.053	0.035	0.035	112.94	216.1	-0.370	3.36

Table S2. The calculated Pearson's correlation coefficients of nine descriptors for the ML of D .

Parament	ρ	nO/V_m	nN/V_m	nC/V_m	nH/V_m	V_m	M	OB	F
PCC- D	0.9381	0.7756	0.7605	0.3410	0.4220	-0.6937	-0.0011	0.1437	-0.2027

Table S3. The setting of the RF model.

NO.	Parameter Name	Parameter settings
1	bootstrap	True
2	ccp_alpha	0.0
3	criterion	mse
4	max_depth	None
5	max_features	auto
6	max_leaf_nodes	None
7	max_samples	None
8	min_impurity_decrease	0.0
9	min_samples_leaf	1
10	n_estimators	200

Table S4. The setting of the SVR model.

NO.	Parameter Name	Parameter settings
1	C	1.0
2	cache_size	200M
3	coef0	0
4	degree	10
5	epsilon	0.1
6	gamma	Scale
7	kernel	rbf
8	max_iter	-1

Table S5. The setting of the MLP model.

NO.	Parameter Name	Parameter settings
1	Input Layer Nodes	9
2	Hidden Layer Nodes	30
3	Output Layer Nodes	1
4	Activation function	tanh
5	Learning rate	0.001
6	Error	0.65×10^{-3}
7	Epochs	2000
8	Optimization solver	Sgd
9	Loss function	MSE

Table S6. The setting of the BPNN model.

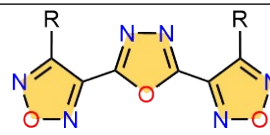
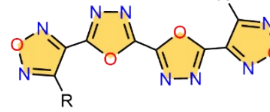
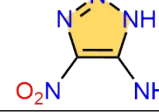
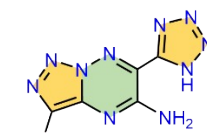
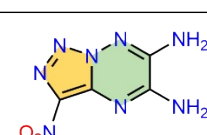
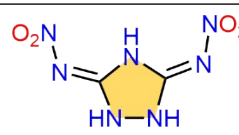
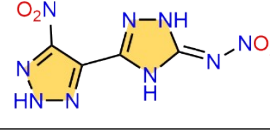
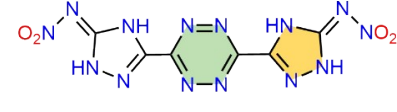
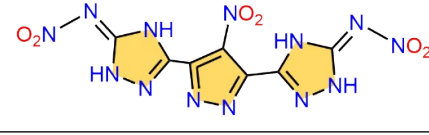
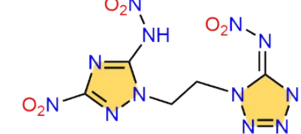
NO.	Parameter Name	Parameter settings
1	Input Layer Nodes	9
2	Hidden Layer Nodes	40
3	Output Layer Nodes	1
4	Activation function	tanh
5	Training function	trainIm
6	Learning rate	0.001
7	Error	0.65×10^{-3}
8	Epochs	4000
9	Optimization solver	RMSprop
10	Loss function	MSE

Table S7. The predicted D ($\text{km}\cdot\text{s}^{-1}$) values of fifteen compounds in the test set.

NO.	Structure	Exp.	BPNN	MLP	RF
1		8.326	8.206	7.997	8.337
2		6.850	7.105	7.467	7.157
3		7.300	7.474	7.633	7.482
4		6.800	6.812	7.209	6.912
5		8.800	8.778	8.305	8.622
6		9.180	9.199	8.293	8.721
7		6.993	7.105	7.322	7.128
8		8.302	8.215	7.708	7.928
9		9.560	9.443	8.615	8.913
10		9.102	9.171	8.434	8.832
11		7.000	7.131	6.914	6.845
12		8.792	8.935	8.533	8.850
13		8.430	8.547	8.268	8.695
14	$\text{H}_3\text{C}-\text{NO}_2$	6.290	6.191	6.372	6.719
15		8.500	8.383	8.563	8.525

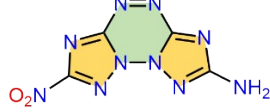
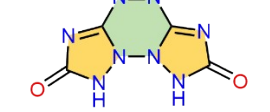
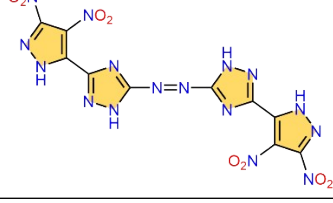
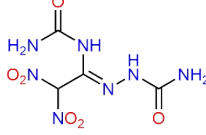
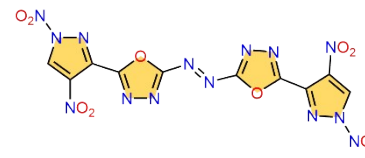
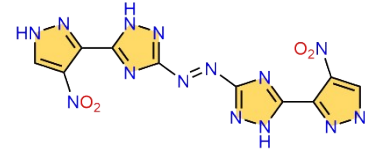
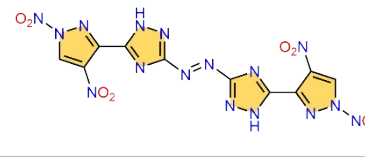
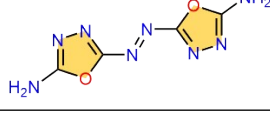
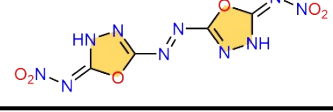
Table S8. The dataset of new test set 1.²⁻¹⁴

NO.	Structure	ρ	nO/ V_m	nN/ V_m	nC/ V_m	nH/ V_m	V_m	M	OB	F
1(P1)		1.71	0.020	0.060	0.040	0.060	99.47	170.1	-0.847	1.84
2(P2)		1.70	0.017	0.060	0.043	0.060	115.95	197.1	-0.933	1.49
3(P3)		1.80	0.028	0.070	0.028	0.028	142.28	256.1	-0.375	3.42
4(P4)		1.77	0.041	0.048	0.034	0.021	145.22	257.0	-0.342	3.48
5		1.91	0.056	0.044	0.033	0.000	180.09	344.0	-0.093	2.11
6		1.83	0.021	0.075	0.032	0.053	93.50	171.1	-0.608	1.94
7		1.87	0.041	0.050	0.041	0.008	241.05	450.0	-0.391	3.25
8		1.81	0.044	0.044	0.039	0.022	181.24	328.0	-0.390	4.53
9		1.82	0.016	0.082	0.033	0.016	122.03	222.1	-0.504	1.52
10		1.80	0.018	0.073	0.037	0.037	108.94	196.1	-0.653	1.66
1		1.800	0.048	0.043	0.034	0.014	207.23	373.0	-0.236	5.28

12		1.82	0.052	0.044	0.030	0.009	229.67	418.0	-0.115	5.68
13		1.91	0.041	0.059	0.035	0.012	170.71	326.1	-0.294	2.65
14		1.92	0.042	0.052	0.042	0.010	190.65	366.0	-0.393	2.29
15		1.21	0.047	0.016	0.016	0.047	63.64	77.0	-0.104	7.06
16		1.82	0.028	0.071	0.028	0.042	70.91	129.1	-0.434	2.76
17		1.75	0.018	0.080	0.027	0.027	112.63	197.1	-0.446	1.74
18		1.77	0.014	0.078	0.036	0.021	140.75	249.1	-0.610	1.28
19		1.81	0.020	0.070	0.040	0.040	100.60	182.1	-0.703	1.78
20		1.83	0.039	0.068	0.019	0.029	103.31	189.1	-0.127	4.79
21		1.88	0.031	0.070	0.031	0.023	128.23	241.1	-0.365	3.34
22		1.88	0.022	0.078	0.034	0.022	178.80	336.1	-0.476	2.53
23		1.92	0.032	0.070	0.032	0.027	184.96	355.1	-0.383	3.50
24		1.80	0.033	0.065	0.027	0.033	183.40	330.1	-0.339	3.79

25		1.70	0.035	0.059	0.023	0.035	85.32	145.1	-0.276	2.97
26		1.88	0.039	0.065	0.026	0.039	77.15	145.1	-0.276	2.97
27		1.86	0.043	0.058	0.029	0.014	138.73	258.0	-0.186	1.60
28		1.90	0.039	0.055	0.039	0.024	126.87	241.1	-0.431	3.29
29		1.76	0.025	0.058	0.042	0.042	120.21	211.1	-0.720	1.45
30		1.73	0.033	0.049	0.041	0.033	122.72	212.1	-0.604	1.47
31		1.82	0.042	0.049	0.035	0.021	141.62	257.0	-0.342	1.24
32		1.89	0.039	0.056	0.039	0.011	178.86	338.1	-0.379	3.25
33		1.88	0.039	0.054	0.039	0.015	202.69	381.1	-0.399	3.89
34		1.88	0.033	0.061	0.039	0.017	179.30	337.1	-0.451	3.24
35		1.76	0.030	0.059	0.037	0.015	135.26	238.1	-0.470	1.37
36		1.83	0.041	0.055	0.034	0.000	146.46	268.0	-0.239	2.75

Table S9. The new dataset of new modified ML model.¹⁵⁻²⁷

NO.	Structure	ρ	nO/ V_m	nN/ V_m	nC/ V_m	nH/ V_m	V_m	M	OB	F
New training set										
1		1.973	0.039	0.052	0.052	0.013	77.56	153.0	-0.575	2.90
2		1.998	0.028	0.085	0.028	0.014	141.19	282.1	-0.284	3.15
3		1.892	0.017	0.085	0.034	0.017	117.39	222.1	-0.504	0.62
4		1.903	0.020	0.078	0.039	0.020	101.99	194.1	-0.577	0.71
5		1.855	0.031	0.062	0.039	0.016	256.67	476.1	-0.470	3.05
6		1.700	0.041	0.048	0.027	0.041	145.92	248.1	-0.322	3.68
7		1.890	0.040	0.055	0.040	0.008	252.94	478.1	-0.368	3.37
8		1.800	0.019	0.065	0.047	0.028	214.53	386.2	-0.787	1.65
9		1.900	0.032	0.064	0.040	0.016	250.59	476.1	-0.470	3.36
10		1.760	0.018	0.072	0.036	0.036	111.42	196.1	-0.653	3.70
11		1.970	0.041	0.069	0.028	0.014	145.21	286.1	-0.168	3.10

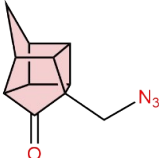
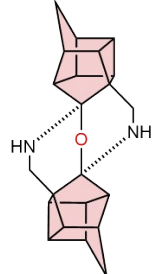
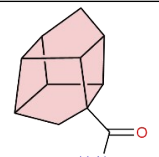
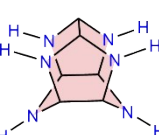
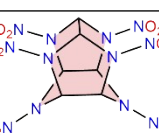
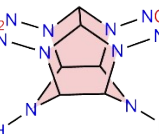
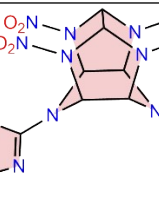
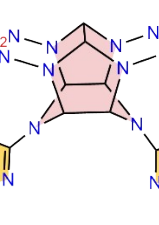
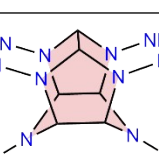
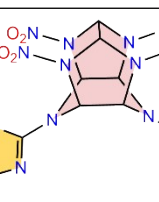
12		1.712	0.009	0.071	0.045	0.036	224.43	384.2	-0.916	-0.46
13		1.920	0.031	0.068	0.037	0.026	191.21	367.1	-0.458	2.26
14		1.860	0.043	0.057	0.028	0.036	140.36	261.1	-0.276	3.33
15		1.990	0.046	0.062	0.031	0.015	129.67	258.0	-0.186	3.44
16		1.862	0.072	0.026	0.026	0.020	151.97	283.0	0.085	2.58
17		1.679	0.070	0.014	0.028	0.028	142.92	240.0	0.000	6.36
18		1.820	0.015	0.087	0.029	0.015	274.86	500.2	-0.448	-0.25
19		1.820	0.011	0.098	0.022	0.011	183.62	334.2	-0.335	-0.19
20		1.85	0.030	0.045	0.060	0.030	134.09	248.1	-0.903	2.72
21		2.12	0.040	0.070	0.040	0.010	199.09	422.1	-0.341	1.98
22		1.86	0.033	0.055	0.044	0.022	180.69	336.1	-0.571	0.22
23		1.92	0.038	0.057	0.038	0.057	210.50	404.2	-0.554	1.55
24		1.75	0.021	0.053	0.053	0.032	188.64	330.1	-0.921	-0.49
25		1.68	0.022	0.056	0.044	0.011	179.81	302.1	-0.689	-0.37

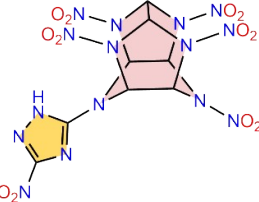
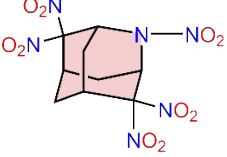
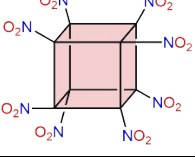
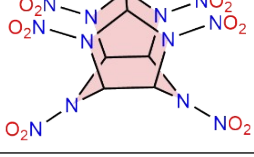
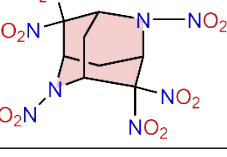
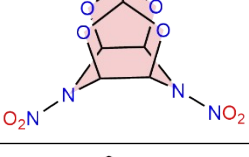
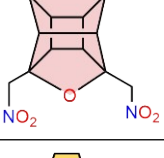
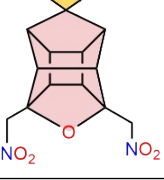
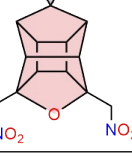
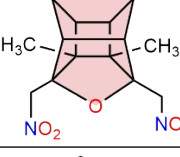
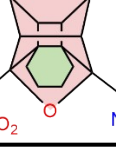
26		1.77	0.036	0.054	0.036	0.009	222.63	394.1	-0.365	2.13
27		1.75	0.033	0.050	0.041	0.025	241.20	422.1	-0.569	1.87
28		1.77	0.021	0.064	0.043	0.021	187.64	332.1	-0.674	-0.38
29		1.83	0.035	0.061	0.035	0.009	230.64	422.1	-0.341	1.98
30		1.79	0.036	0.054	0.036	0.036	223.53	400.1	-0.480	1.62
31		1.92	0.039	0.058	0.039	0.010	205.24	394.1	-0.365	2.13
32		1.810	0.012	0.060	0.060	0.048	165.83	300.2	-1.173	-0.58
33		1.790	0.011	0.076	0.043	0.033	184.46	330.2	-0.824	-0.42
34		1.870	0.027	0.071	0.036	0.018	224.67	420.1	-0.457	1.96
35		1.680	0.019	0.065	0.037	0.028	215.57	362.2	-0.663	0.17
36		1.760	0.035	0.055	0.035	0.014	288.69	508.1	-0.378	2.85
37		1.900	0.044	0.057	0.032	0.006	314.77	598.1	-0.187	3.78

38		1.690	0.011	0.078	0.034	0.011	178.78	302.1	-0.583	-0.29
39		1.830	0.027	0.072	0.032	0.009	221.92	406.1	-0.355	1.72
40		1.740	0.018	0.072	0.036	0.012	166.73	290.1	-0.552	-0.30
41		1.830	0.041	0.049	0.041	0.008	245.92	450.0	-0.391	3.25
42		1.820	0.019	0.084	0.028	0.019	215.48	392.2	-0.408	1.78
43		1.760	0.018	0.081	0.027	0.009	221.68	390.2	-0.369	1.83
44		1.650	0.020	0.069	0.029	0.020	203.72	336.1	-0.476	-0.30
45		1.640	0.030	0.059	0.026	0.030	270.83	444.2	-0.360	-0.31
46		1.870	0.033	0.058	0.042	0.017	239.63	448.1	-0.500	3.24
47		1.806	0.027	0.067	0.033	0.040	149.57	270.1	-0.533	2.59
48		1.650	0.033	0.060	0.020	0.033	149.75	247.1	-0.227	-0.28

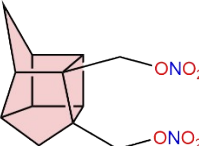
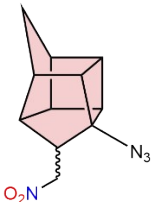
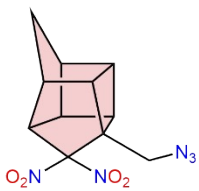
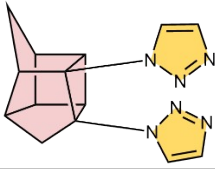
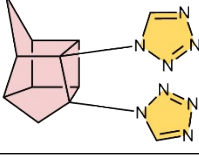
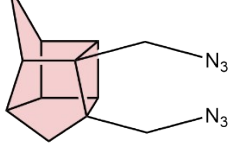
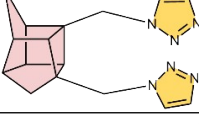
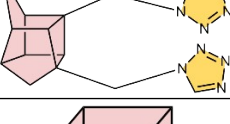
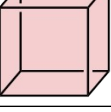
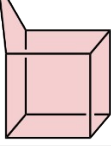
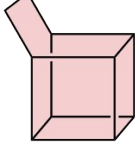
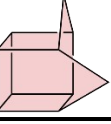
49		1.680	0.024	0.071	0.024	0.024	253.68	426.2	-0.338	-0.26
50		1.770	0.032	0.064	0.027	0.032	186.51	330.1	-0.339	3.33
51		1.780	0.017	0.084	0.025	0.034	119.17	212.1	-0.453	1.94
52		1.740	0.024	0.073	0.024	0.024	122.47	213.1	-0.338	1.61
53		1.710	0.019	0.077	0.026	0.019	156.21	267.1	-0.389	-0.26
54		1.680	0.022	0.065	0.033	0.022	91.70	154.1	-0.519	-0.32
55		1.794	0.045	0.056	0.023	0.011	177.28	318.0	-0.050	4.83
56		1.757	0.043	0.053	0.027	0.011	187.84	330.0	-0.145	4.62
57		1.680	0.020	0.079	0.020	0.020	101.24	170.1	-0.282	-0.22
58		1.795	0.021	0.078	0.028	0.021	141.01	253.1	-0.411	-0.27
59		1.678	0.046	0.023	0.046	0.058	172.86	290.1	-0.717	5.042

60		1.645	0.042	0.024	0.048	0.060	166.61	274.1	-0.817	5.336
61		1.850	0.032	0.065	0.032	0.040	247.66	458.2	-0.454	3.792
62		2.050	0.019	0.019	0.114	0.105	209.86	430.2	-2.045	-1.017
63		1.580	0.025	0.013	0.076	0.088	158.30	250.1	-1.727	2.249
64		1.440	0.000	0.036	0.071	0.083	168.19	242.2	-2.048	-0.981
65		1.560	0.000	0.038	0.077	0.100	130.24	203.2	-2.087	-1.015
66		1.360	0.016	0.000	0.085	0.085	128.74	175.1	-2.330	-0.607
67		1.520	0.034	0.011	0.063	0.052	174.38	265.1	-1.238	3.608
68		1.590	0.029	0.007	0.079	0.079	139.04	221.1	-1.701	2.120
69		1.400	0.025	0.010	0.065	0.080	200.09	280.1	-1.656	1.919
70		1.480	0.032	0.014	0.059	0.068	219.67	325.1	-1.304	3.441
71		1.500	0.013	0.013	0.085	0.091	153.43	230.1	-2.155	-0.543

72		1.350	0.007	0.020	0.074	0.067	148.24	200.1	-2.079	-0.500
73		1.300	0.004	0.008	0.087	0.087	254.02	330.2	-2.616	-1.249
74		1.370	0.008	0.008	0.086	0.102	127.83	175.1	-2.512	-0.678
75		1.570	0.000	0.056	0.056	0.112	107.12	168.2	-1.712	-0.892
76		1.970	0.054	0.054	0.027	0.027	222.37	438.1	-0.110	6.249
77		1.870	0.043	0.054	0.032	0.043	186.15	348.1	-0.368	5.099
78		1.870	0.041	0.057	0.033	0.033	246.05	460.1	-0.348	4.673
79		1.840	0.038	0.058	0.032	0.032	312.04	574.2	-0.362	4.376
80		1.720	0.022	0.065	0.032	0.076	185.01	318.2	-0.754	2.475
81		1.840	0.039	0.058	0.031	0.035	258.23	475.1	-0.354	4.512

82		1.900	0.045	0.056	0.030	0.026	265.84	505.1	-0.238	5.209
83		1.813	0.050	0.030	0.045	0.040	198.59	360.0	-0.533	3.993
84		1.979	0.068	0.034	0.034	0.000	234.42	463.9	0.000	6.682
85		2.040	0.076	0.040	0.020	0.020	300.96	614.0	0.208	4.459
86		1.960	0.058	0.038	0.038	0.038	208.18	408.0	-0.314	5.882
87		1.990	0.061	0.030	0.046	0.046	131.67	262.0	-0.427	3.196
88		1.600	0.012	0.029	0.076	0.082	170.11	272.2	-1.822	2.021
89		1.590	0.010	0.024	0.083	0.097	205.18	326.2	-2.060	1.418
90		1.510	0.010	0.025	0.076	0.081	197.48	298.2	-1.932	1.719
91		1.370	0.009	0.023	0.068	0.082	219.13	300.2	-1.972	1.666
92		1.460	0.009	0.022	0.076	0.090	223.45	326.2	-2.060	1.418

93		1.410	0.009	0.022	0.074	0.070	228.50	322.2	-1.986	1.513
94		1.460	0.048	0.009	0.044	0.048	229.47	335.0	-0.692	0.616
95		1.490	0.014	0.027	0.068	0.068	146.39	218.1	-1.687	2.808
96		1.650	0.015	0.030	0.076	0.076	132.19	218.1	-1.687	2.808
97		1.390	0.047	0.007	0.040	0.047	274.12	381.0	-0.651	1.526
98		1.540	0.013	0.025	0.075	0.088	159.84	246.2	-1.885	2.285
99		1.500	0.012	0.024	0.073	0.085	164.11	246.2	-1.885	2.285
100		1.580	0.013	0.026	0.077	0.090	155.80	246.2	-1.885	2.285
101		1.580	0.017	0.034	0.063	0.063	174.14	275.1	-1.425	3.612
102		1.580	0.013	0.039	0.064	0.064	155.78	246.1	-1.495	3.910

103		1.590	0.012	0.035	0.070	0.081	172.44	274.2	-1.692	3.328
104		1.550	0.025	0.012	0.074	0.087	161.37	250.1	-1.727	0.650
105		1.660	0.030	0.024	0.065	0.065	168.13	279.1	-1.290	2.127
106		1.370	0.039	0.017	0.039	0.039	357.71	490.1	-0.686	-0.536
107		1.570	0.041	0.027	0.041	0.041	293.04	460.1	-0.626	-0.489
108		1.440	0.043	0.019	0.037	0.043	323.65	466.1	-0.584	-0.510
109		1.520	0.047	0.016	0.042	0.047	382.93	582.1	-0.632	-0.537
110		1.530	0.044	0.022	0.039	0.044	360.84	552.1	-0.580	-0.498
111		1.290	0.030	0.030	0.030	0.030	266.73	344.1	-0.558	-0.436
112		1.340	0.030	0.033	0.030	0.033	300.08	402.1	-0.557	-0.435
113		1.190	0.026	0.031	0.026	0.031	386.67	460.1	-0.556	-0.435
114		1.520	0.033	0.040	0.033	0.040	302.72	460.1	-0.556	-0.435

115		1.070	0.023	0.028	0.023	0.028	430.04	460.1	-0.556	-0.435
116		1.370	0.030	0.036	0.030	0.036	335.87	460.1	-0.556	-0.435
117		1.450	0.035	0.031	0.035	0.031	453.88	658.1	-0.559	-0.437
118		1.340	0.031	0.031	0.031	0.031	641.94	860.2	-0.558	-0.436

New test set 2

1(P5)		1.790	0.024	0.078	0.024	0.024	166.55	298.1	-0.322	-0.25
2(P6)		1.570	0.025	0.025	0.062	0.075	160.59	252.1	-1.396	2.975
3		1.880	0.022	0.078	0.034	0.022	178.80	336.1	-0.476	2.53
4		1.8	0.027	0.059	0.043	0.016	185.05	333.1	-0.600	-0.36
5		1.89	0.034	0.057	0.045	0.011	176.75	334.1	-0.527	0.26
6		1.85	0.038	0.056	0.038	0.009	213.01	394.1	-0.365	2.13

7		1.860	0.041	0.050	0.041	0.008	241.96	450.0	-0.391	3.25
8		1.820	0.014	0.090	0.028	0.014	145.13	264.1	-0.424	-0.24
9		1.880	0.034	0.059	0.042	0.017	238.35	448.1	-0.500	3.24
10		1.770	0.026	0.066	0.033	0.039	152.61	270.1	-0.533	2.59
11		1.873	0.015	0.083	0.038	0.023	133.01	249.1	-0.610	1.28
12		1.490	0.020	0.024	0.063	0.073	204.81	305.2	-1.547	1.782
13		1.960	0.041	0.062	0.031	0.052	192.93	378.1	-0.381	4.661
14		1.790	0.028	0.055	0.042	0.069	144.21	258.1	-0.806	3.148
15		1.440	0.009	0.022	0.075	0.088	226.55	326.2	-2.060	1.418
16		1.390	0.022	0.022	0.055	0.066	181.38	252.1	-1.396	2.975
17		1.480	0.040	0.024	0.040	0.040	252.74	374.1	-0.642	-0.501

Table S10. The dataset of new energetic compounds.

NO.	Name	ρ	nO/V_m	nN/V_m	nC/V_m	nH/V_m	V_m	M	OB	F
1	NEC1	1.80	0.054	0.039	0.031	0.047	128.93	232.1	-0.414	3.07
2	NEC2	1.81	0.050	0.044	0.031	0.044	160.82	291.1	-0.357	3.76
3	NEC3	1.79	0.063	0.031	0.031	0.031	127.42	228.1	-0.421	3.18
4	NEC4	1.77	0.053	0.035	0.035	0.041	170.11	301.1	-0.505	3.59
5	NEC5	1.89	0.077	0.031	0.026	0.015	195.30	369.1	-0.238	3.44
6	NEC6	1.88	0.078	0.029	0.024	0.020	204.33	384.1	-0.250	3.29
7	NEC7	1.94	0.055	0.049	0.031	0.006	162.38	315.0	-0.127	4.15
8	NEC8	1.91	0.052	0.046	0.035	0.017	172.27	329.0	-0.267	3.89
9	NEC9	1.91	0.073	0.034	0.021	0.009	233.47	445.9	0.215	4.09
10	NEC10	1.92	0.076	0.032	0.020	0.016	249.96	479.9	0.233	3.15
11	NEC11	1.92	0.035	0.056	0.045	0.042	287.59	552.2	-0.637	5.64
12	NEC12	1.94	0.036	0.061	0.040	0.030	328.96	638.2	-0.476	6.15

Table S11. The D prediction results of three isomers

NO.	Structure ^{a)}	$\rho/\text{g}\cdot\text{cm}^{-3}$	$D/\text{km}\cdot\text{s}^{-1}$	Predicted $D/\text{km}\cdot\text{s}^{-1}$	Relative error /%
I1		1.800	8.574 ^{b)}	8.941	4.280
		1.880	8.952	8.998	0.514
I2		1.800	8.990 ^{b)}	8.941	-0.545
		1.777	8.916	8.922	0.067
I3		1.800	8.935 ^{b)}	8.941	0.067
		1.795	8.917	8.937	0.224

a) I1 is 3 from Yu's work (Z. Anorg. Allg. Chem. 2020); I2 and I3 is N8L and N8B from Lai's work (Chem. Eng. J. 2021).

b) These data were computed by EXPLO5.

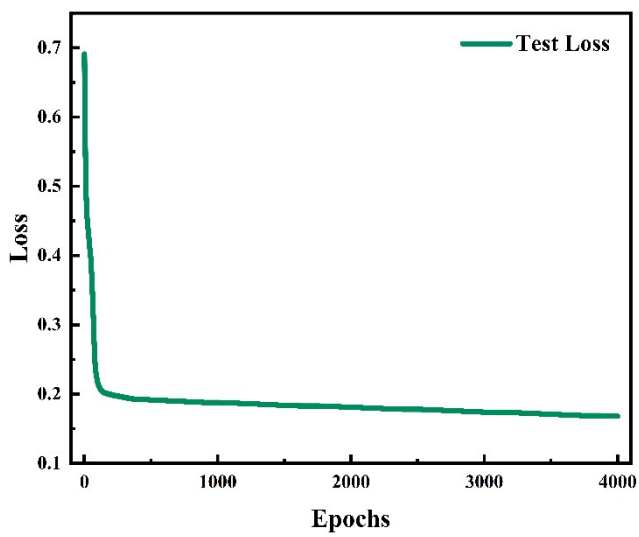


Figure S1. The loss function of ML models

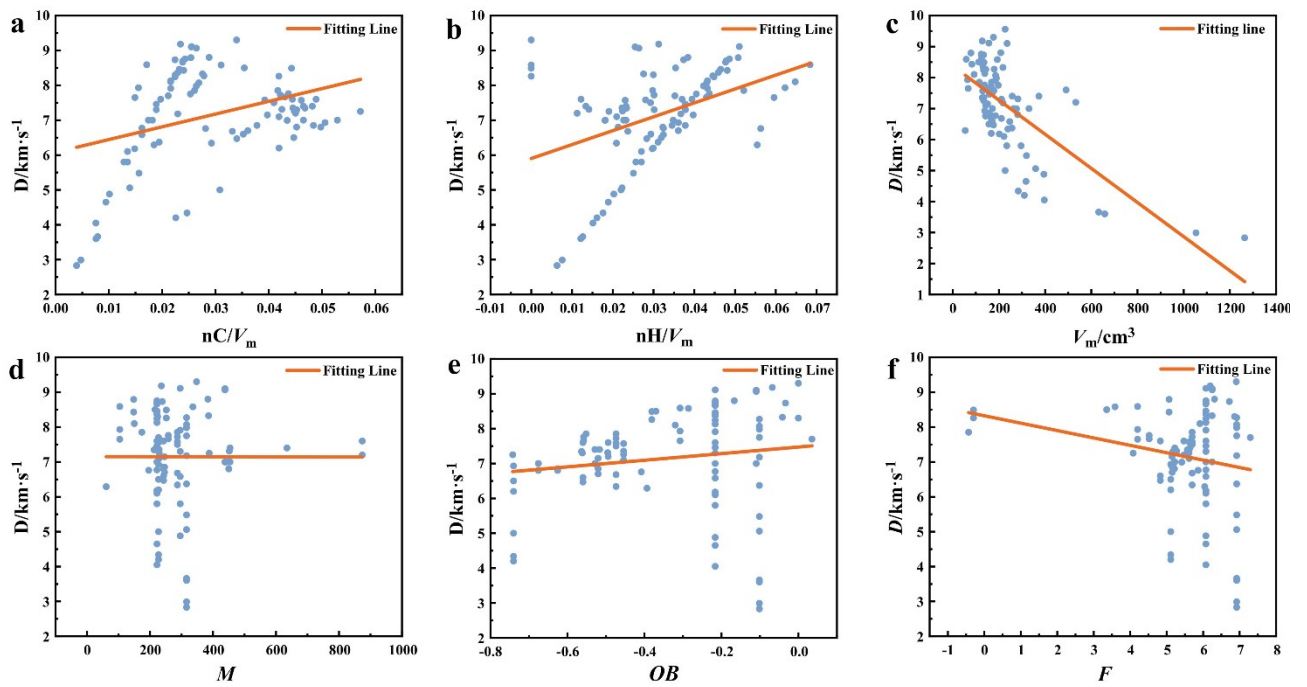


Figure S2. The relationships between nC/V_m , nH/V_m , V_m , M , OB , F and experimental D results

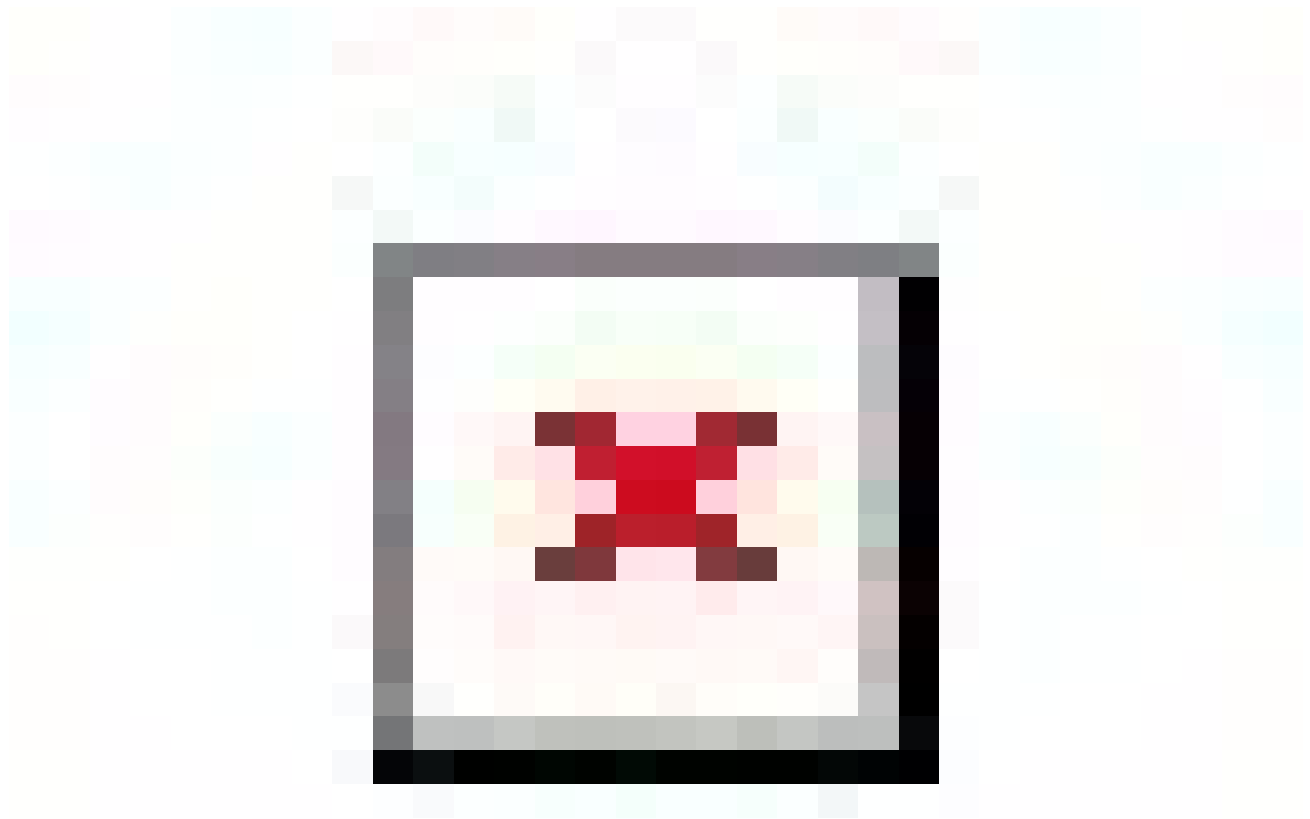


Figure S3. The scatter graph of the training/test set showing the D predicted vs experimental values:

(a)BPNN, (b)MLP, (c)RF and (d)SVR models

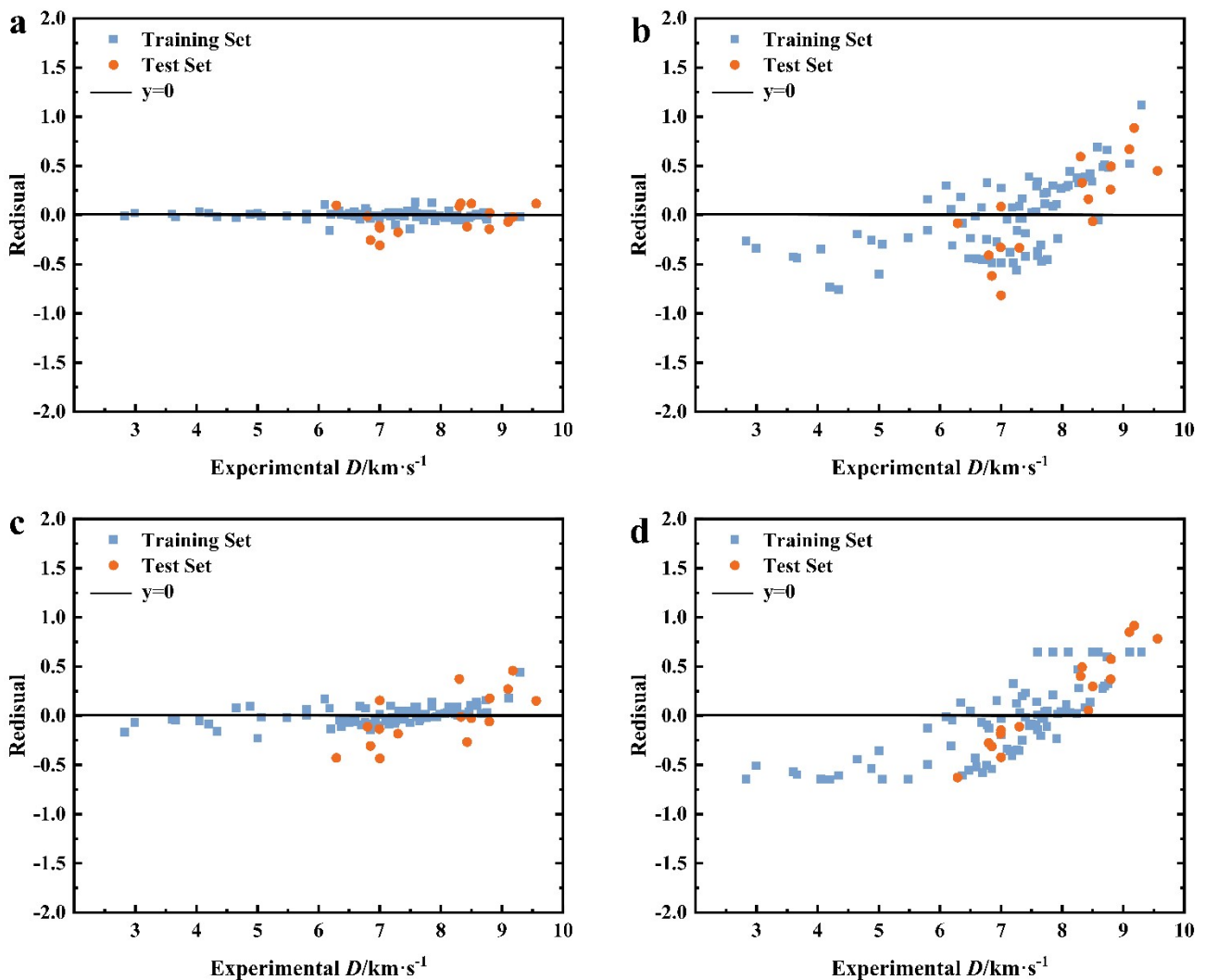


Figure S4. The predicted residual plot of (a)BPNN, (b)MLP, (c)RF and (d)SVR models for the D

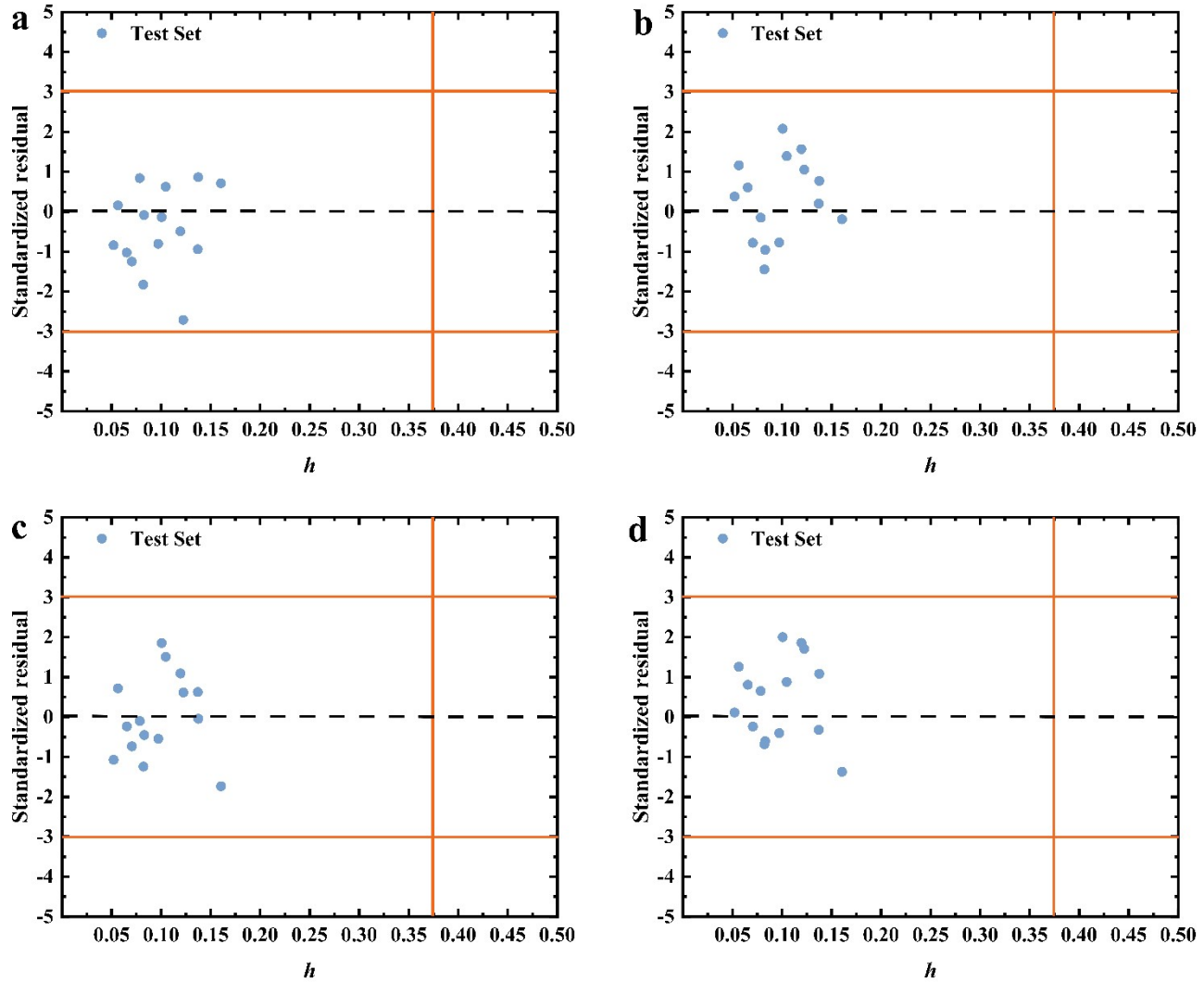


Figure S5. The Williams plot of (a)BPNN, (b)MLP, (c)RF and (d)SVR models for the test set of the D

References

- 1 X. Xiong, M.D. thesis, Southwest University of Science and Technology, 2020.
- 2 L. Zhai, F. Bi, Y. Luo, N. Wang, J. Zhang , B. Wang, *Scientific Reports*, 2019, **9**, 4321.
- 3 Y. Tang, W. Huang, G.H. Imler, D.A. Parrish, J.M. Shreeve, 2020, **142**, 7153–7160.
- 4 H. Li, L. Zhang, N. Petrutik, K. Wang, Q. Ma, D. Shem-Tov, F. Zhao, M. Gozin, *ACS Central Science*, 2020, **6**, 54–75.
- 5 W. Huang, Y. Tang, G.H. Imler, D.A. Parrish, J.M. Shreeve, 2020, *Journal of the American Chemical Society*, 2020, **142**, 3652–3657.
- 6 S. Feng, P. Yin, C. He, S. Pang, J. M. Shreeve, *J. Mater. Chem. A*, 2021, **9**, 12291–12298.
- 7 M. Reichel, B. Krumm, Y. V. Vishnevskiy, S. Blomeyer, J. Schwabedissen, H.-G. Stammmer, K. Karaghiosoff, N. W. Mitzel, *Angew. Chem. Int. Ed.*, 2019, **58**, 18557–18561.
- 8 M. Reichel, B. Krumm, Y. V. Vishnevskiy, S. Blomeyer, J. Schwabedissen, H.-G. Stammmer, K. Karaghiosoff, N. W. Mitzel, *Angew. Chem. Int. Ed.*, 2019, **58**, 18557–18561.
- 9 Y. Wang, L. Hu, S. Pang, J. M. Shreeve, *J. Mater. Chem. A*, 2023, **11**, 13876–13888.
- 10 W. Huang, Y. Tang, G. H. Imler, D. A. Parrish, J. M. Shreeve, *J. Am. Chem. Soc.*, 2020, **142**, 3652–3657.
- 11 C. Li, T. Zhu, C. Lei, G. Cheng, C. Xiao, H. Yang, *J. Mater. Chem. A*, 2023, **11**, 12043–12051.
- 12 R. Yang, Z. Dong, Y. Liu, Y. Liu, H. Li, G. Zhang, Z. Ye, *Chem. Eng. J.*, 2022, **429**, 132503.
- 13 J. Ma, A. K. Chinnam, G. Cheng, H. Yang, J. Zhang, J. M. Shreeve, *Angew. Chem-ger. Edit.*, 2021, **133**, 5557–5564.
- 14 H. Dou, P. Chen, L. Hu, C. He, S. Pang, *Chem. Eng. J.*, 2022, **444**, 136708.
- 15 S. Banik, A. Kumar Yadav, P. Kumar, V. D. Ghule, S. Dharavath, *Chem. Eng. J.*, 2022, **431**, 133378.
- 16 X. Jiang, Y. Yang, H. Du, B. Yang, P. Tang, B. Wu, C. Ma, *Dalton Trans.*, 2023, **52**, 5226–5233.
- 17 Y. Li, X. Wang, M. Xue, *New J. Chem.*, 2023, **47**, 19191–19201.
- 18 L. Mallick, S. Lal, S. Reshma, I. N. N. Namboothiri, A. Chowdhury, N. Kumbhakarna, *New J. Chem.*, 2017, **41**, 920–930.
- 19 S. Lal, S. Rao Cheekatla, A. Suresh, N. Ayyagari, L. Mallick, G. Pallikonda, P. Desai, P. Ahirwar, A. Chowdhury, N. Kumbhakarna, I. N. N. Namboothiri, *Chemistry – A European Journal*, 2024, **30**, e202401265.
- 20 L. Zhu, Q. Zhou, W. Wang, H. Li, B. Li, Y. Zhang, J. Luo, *Energetic Materials Frontiers*, 2024, DOI:10.1016/j.enmf.2024.06.005.
- 21 J. Cai, C. Xie, J. Xiong, J. Zhang, P. Yin, S. Pang, *Chem. Eng. J.*, 2022, **433**, 134480.

- 22 S. Banik, P. Kumar, V. D. Ghule, S. Khanna, D. Allimuthu, S. Dharavath, *J. Mater. Chem.a*, 2022, **10**, 22803–22811.
- 23 L. Zhang, Q. Lang, M. Zhu, X. Zhang, S. Jiang, M. Lu, Q. Lin, *ACS Appl. Mater. Interfaces*, 2024, **16**, 10211–10217.
- 24 S. Kotha, M. Salman, S. Lal, S. Rao Cheekatla, S. Ansari, *Asian J. Org. Chem.*, 2023, **12**, e202300060.
- 25 Y. Xu, L. Ding, D. Li, Z. Xu, P. Wang, Q. Lin, M. Lu, *J. Mater. Chem. A*, 2024, **12**, 17714–17729.
- 26 P. Maksimowski, T. Gołofit, *J. Energ. Mater.*, 2013, **31**, 224–237.
- 27 T. Hou, H. Ruan, G. Wang, J. Luo, *Eur. J. Org. Chem.*, 2017, **2017**, 6957–6960.